nochemistry 4, 11.
Scatchard, G. (1949), *Ann. N.Y. Acad. Sci. 51,* 660.
Schlessinger, J., Steinberg, I. Z., and Pecht, I. (1974), *J. Mol. Biol. 87,* 725.
Shimizu, A., Watanabe, S., Yamamura, Y., and Putnam, F. W. (1974), *Immunochemistry 11,* 719.
Sledge, C. R., and Bing, D. H. (1973), *J. Biol. Chem. 248,* 2818.
Voss, E. W., Russell, W. J., and Sigel, M. M. (1969), *Biochemistry 8,* 4866.
Voss, E. W., and Sigel, M. M. (1972), *J. Immunol. 109,* 665.
Warner, N. L. (1974), *Adv. Immunol. 19,* 67.
Watanabe, S., Barnikol, H. V., Horn, J., and Hilschmann, N. (1973), *Hoppe-Seyler's Z. Physiol. Chem. 354,* 1505.
Weber, K., and Osborn, M. (1969), *J. Biol. Chem. 244,* 4406.
Werner, T. C., Bunting, J. R., and Cathou, R. E. (1972), *Proc. Natl. Acad. Sci. U.S.A. 69,* 795.
Zagyansky, Y. (1975), *Arch. Biochem. Biophys. 166,* 371.
Zikán, J., and Bennett, J. C. (1973), *Eur. J. Immunol. 3,* 415.
Zikán, J., and Miler, I. (1974), *Immunochemistry 11,* 115.

Conformation of Immunoglobulin M. 2. Nanosecond Fluorescence Depolarization Analysis of Segmental Flexibility in Anti-ϵ-1-Dimethylamino-5-naphthalenesulfonyl-L-lysine Anti-Immunoglobulin from Horse, Pig, and Shark†

David A. Holowka‡ and Renata E. Cathou*

ABSTRACT: The rotational motions of immunoglobulin M (IgM) were investigated by the nanosecond fluorescence depolarization technique. The fluorophore ϵ-1-dimethylamino-5-naphthalenesulfonyl-L-lysine (DNS-lysine) was specifically bound in the combining sites of anti-DNS IgM antibodies from the horse, pig, and nurse shark. Fluorescence lifetime analysis showed the presence of a long lifetime component (21–27 ns) with antibodies from all three species. With the mammalian antibodies, the fluorophore appeared to be rigidly bound in the combining sites as judged by the presence of induced circular dichroism of DNS-lysine (equine antibodies) and single exponential anisotropy decay of the isolated Fabμ fragments (equine and porcine antibodies). The small amount of available purified nurse shark antibody did not allow preparation of fragments or induced circular dichroism measurements to directly determine rigidity of fluorophore binding. However, at least some of the hapten must have been rigidly bound since long rotational correlation times were measured for the shark DNS-lysine–anti-DNS complexes. When the emission anisotropy of the fluorophore–anti-DNS IgM complexes was measured as a function of time, it was found that all three antibody species exhibited restricted segmental flexibility in the nanosecond time range. Moreover, when the equine anti-DNS IgM was exposed to 1 M acetic acid for 1 h, the antibody underwent a conformational change which resulted in an increase in its overall flexibility. Comparison of the rotational correlation times of native equine IgM and of proteolytic fragments indicated that flexibility of IgM consists of either hindered rotation of the Fab′μ segment or a combination of at least two modes of motion: rotation of Fabμ and/or Fab′μ and bending of the entire $(Fab')_{2}\mu$ region as a unit. Similar modes of flexibility also occur in native porcine IgM. In acid exposed equine IgM, the major contribution to depolarization is from independent rotation or wagging of the Fab′μ segments. Thus, acid apparently causes a conformational change in or near the Cμ2 domains. In contrast, flexibility in nurse shark IgM appears to involve only bending of $(Fab')_{2}\mu$ as a unit. Our results suggest that segmental flexibility is an essential functional feature of all IgM antibodies and that control of this flexibility through domain interactions may play an important role in such conformationally sensitive functions as complement fixation.

The question of segmental flexibility in the immunoglobulins has been the subject of considerable attention since it was first proposed for immunoglobulin G (IgG)[1] by Noelken et al. (1965) (for reviews, see Metzger, 19 ; Cathou and Dorrington, 1975). Electron microscopic studies have shown that the Fab segments can take on different orientations with re-

† From the Department of Biochemistry and Pharmacology, Tufts University School of Medicine, Boston, Massachusetts 02111. *Received December 31, 1975.* Supported by U.S. Public Health Service Grant AI-10115 and American Heart Association Grant 72-671. R.E.C. was a Senior Investigator of the Arthritis Foundation. Taken in part from a dissertation submitted by D.A.H. in partial fulfillment of the requirements for the degree of Doctor of Philosophy, Tufts University, Medford, Massachusetts, 1975.

‡ Present address: Department of Chemistry, Cornell University, Ithaca, New York, 14853.

[1] Abbreviations used: DNS-lysine, ϵ-1-dimethylamino-5-naphthalenesulfonyl-L-lysine; anti-DNS, antibodies elicited to the DNS-lysine hapten which show measurable binding of the DNS determinant; DNS–HSA, DNS covalently conjugated to human serum albumin; dansic acid, dimethylaminonaphthalenesulfonic acid; KLH, keyhole limpet hemocyanin; Tris, tris(hydroxymethyl)aminomethane; 2-ME, 2-mercaptoethanol; C1q, first component of complement; IgM, immunoglobulin M; IgG, immunoglobulin G.

spect to the Fc region in IgG (Valentine and Green, 1967) and in IgM (Feinstein et al., 1971). In the case of free IgM, the Fabμ segments generally appear to project radially from the central (Fc)$_5\mu$ disk in a stellar configuration. In contrast, in the case of anti-*Salmonella* IgM attached to *Salmonella* flagella, the Fabμ arms appear to be bent out of the (Fc)$_5\mu$ plane in order to bind to the flagellum surface, and it has been suggested that this altered conformation may be necessary for enhanced complement fixation (Feinstein et al., 1971). Functionally, flexibility of the Fabμ segments would be expected to have advantages in the formation of multivalent antigen–antibody complexes, and might well play a more subtle role in the transfer of a signal from the antigen binding sites on the Fab segments to the Fc region to trigger effector processes such as the binding of the first component of complement.

In solution, the most widely used approach to study this question of flexibility in the immunoglobulins has been fluorescence depolarization. Classically, the method of choice has been steady-state polarization, in which the dependence of macromolecular Brownian rotation on solution viscosity is utilized to determine a mean rotational correlation time ($\bar{\phi}$) for the macromolecule (Weber, 1952 a,b; Gottlieb and Wahl, 1963). Unfortunately, the results, as well as the interpretations, of a number of studies on IgG disagree (see Cathou et al., 1974; Holowka, 1975). More recently, nanosecond depolarization studies have been carried out by Yguerabide et al. (1970) on DNS-lysine–anti-DNS IgG complexes. The results from these studies were interpreted most readily in terms of the presence of a flexible hinge joining Fab to Fc which allows the Fab segments some rotational freedom in the nanosecond time range (Yguerabide et al., 1970).

Results from several steady-state fluorescence depolarization studies of IgM also suggest internal flexibility. Metzger et al. (1966), using a DNS-conjugated human Waldenstrom IgM, found low values for $\bar{\phi}$, i.e., 27 ns. Zagyansky et al. (1972), using three different DNS-conjugated Waldenstrom macroglobulins, also obtained low values of $\bar{\phi}$, i.e., 27–47 ns. Knopp and Weber (1969), employing a pyrenebutyryl conjugate of human IgM, obtained a value of $\bar{\phi}$ = 330 ns, which they interpreted as rotation of the entire macromolecule, although they pointed out the presence of additional degrees of freedom with much shorter correlation times. We previously reported a value of $\bar{\phi}$ of 82 ns for equine anti-DNS IgM with DNS-lysine bound rigidly in the combining site, which we interpreted as evidence for some flexibility (Holowka and Cathou, 1974; Cathou et al., 1974). In a phylogenetic comparison, Zagyansky has concluded from steady-state polarization studies of IgM from lower vertebrates that the degree of over-all flexibility decreases with the level of phylogeny (Zagyansky and Ivannikova, 1974; Zagyansky, 1975).

We have now extended our studies on equine anti-DNS IgM by the use of the single photon nanosecond fluorescence depolarization technique (Yguerabide, 1972) and have indeed found that the Fab'μ segment, and possibly also the entire (Fab')$_2\mu$ region, has some freedom to rotate independently of the whole IgM, but that this freedom is partially restricted by an acid-sensitive conformation. Porcine anti-DNS IgM appears to exhibit a similar degree of internal rotational freedom. In contrast, nurse shark anti-DNS IgM exhibits more restricted flexibility which we have interpreted as primarily bending of the entire (Fab')$_2\mu$ region as a unit.

Materials and Methods

Characterization of IgM and Proteolytic Fragments. Anti-DNS IgM antibodies from the horse, pig, and nurse shark were elicited and purified as described in the preceding paper (Holowka and Cathou, 1976). Equine (Fab')$_2\mu$, Fab'μ (pepsin), and Fabμ (papain) fragments were prepared from acid-eluted antibody and characterized as described previously (Holowka and Cathou, 1976). Porcine Fabμ and (Fc)$_5\mu$ fragments were prepared from anti-DNS IgM by pepsin digestion at 37 °C for 12 h according to published methods (Beale, 1974; Zikăn and Miler, 1974). The digest was fractionated on a Sepharose 4B (Pharmacia) column (2.5 × 75 cm) in 0.02 M Tris–0.15 M NaCl buffer, pH 8. Porcine (Fc)$_5\mu$ was conjugated with DNS-Cl by the method of Weber (1952b) in 0.1 M carbonate buffer, pH 9.2, for 10 h at 4 °C. After exhaustive dialysis, the extent of DNS conjugation to (Fc)$_5\mu$ was measured using a molar extinction coefficient of 4.6×10^3 at 330 nm (Parker et al., 1967). Protein concentrations for all IgM and fragment solutions were determined using an extinction coefficient at 280 nm of 1.35 for a 1.0 mg/ml solution (Kim and Karush, 1973). Samples for nanosecond fluorescence analysis were routinely titrated with a molar excess of DNS-lysine, dialyzed overnight vs. 0.02 M Tris–0.15 M NaCl buffer, pH 8.0, to remove any unbound DNS-lysine and filtered with a 0.22-μm MF-Millipore filter (Millipore Corp., Bedford, Mass.). Protein concentrations in these experiments ranged from 0.11 to 1.75 mg/ml; no depolarization dependence on concentration was observed in this range. For all depolarization results presented, experiments were performed two or more times to ensure reproducibility, and in all cases except that of porcine (Fc)$_5\mu$, at least two different preparations were employed.

Nanosecond Fluorescence Measurements. The time course of fluorescence emission was measured by the single photon counting technique (Yguerabide, 1972) using the basic Ortec 9200 system (Ortec, Inc., Oak Ridge, Tenn.) with some modifications. The Ortec spark-gap lamp (Model 9352) was pulsed in air at about 25 kHz, and had a width at half-maximum of 3 ns. The sample compartment was a modified Aminco-Bowman fluorimeter compartment mounted on an optical bench and was enclosed, along with the lamp, an RCA 8850 photomultiplier, and housing, in a 74 × 54 × 42 cm light-tight box. Light pulses from the lamp were focused on the center of the sample compartment with a short focal length lens (Oriol Corp., Stamford, Conn.), and emitted fluorescence at 90° to the excitation light path was similarly focused on the photomultiplier window. The intensity of exciting and emitted light was controlled by means of slits mounted on the cuvette holder. Exciting and emitted light were linearly polarized with manually rotated Polacoat Ultraviolet Polarizing Filters (Polacoat, Inc., Cincinnati, Ohio), which were mounted on the cuvette holder. It was found that in order to attain a degree of polarization which was comparable to that measured by steady-state fluorescence (see below), the proper collimation of light by adjustment of the lenses and slits was important since lower values of polarization were observed at higher light intensities. Emitted light was filtered with a 500-nm narrow band interference filter with a 10-nm spectral band width (Oriel Corp. G522-5000), which was placed after the collimating emission lens. For most depolarization experiments reported here, excitation pulses were filtered by means of a 355-nm glass band pass filter with a 54-nm spectral band width (Oriel G774-3550) which was placed between the collimating lens and the excitation polarizer. In studies of the excitation wavelength dependence of both the fluorescence lifetime and the nanosecond depolarization, three-cavity narrow bandpass filters (Ditric Optics, Inc., Sacramento, Calif.) were employed.

Less than 2% of the photons could be attributed to excitation light from the lamp scattered by the IgM solution in the absence of DNS-lysine.

Nanosecond decay data were collected and analyzed by methods which were similar to those employed by Yguerabide et al. (1970). The exciting light pulses were vertically polarized, and emitted photons were collected with the emission polarizer's axis of polarization oriented either vertically (VV) or horizontally (VH). For fluorescence lifetime measurements, the polarization axis of the emission polarizer was oriented at 55° from the vertical direction to yield completely unpolarized emission (Yguerabide, 1972).

Single photon emission was selected by means of a linear channel (Ortec, Inc.), and timing of the photon emission by the time-to-amplitude converter (TAC) was calibrated by a fast pulse generator (Ortec, Model 462). Output from the TAC was detected and stored in a Series 1100 multichannel analyzer (Nuclear Data, Chicago, Ill.) and then printed out on paper tape and hard copy with a Model 33RO teletypewriter (Teletype Corp., Skokie, Ill.).

For a given nanosecond depolarization experiment, about 3×10^7 photons was accumulated for each of the two polarizer positions, VV and VH, so that with the counting efficiency employed (ca. 3–10%), the entire experiment took about 10–24 h. During this time the sample temperature was maintained at 25 ± 1 °C and no aggregation or denaturation of the proteins could be detected.

Calculation of the Nanosecond Depolarization Decay Curves. Emission anisotropy (A) was calculated as a function of time from the raw experimental data by the standard equation:

$$A(t) = \frac{f_\parallel(t) - f_\perp(t)}{f_\parallel(t) + 2f_\perp(t)} \tag{1}$$

where $f_\parallel(t)$ and $f_\perp(t)$ are the fluorescence intensities of the vertically and horizontally polarized emission components, respectively, as a function of time, t (Yguerabide, 1972). Because the lamp intensity and rate vary slightly during the course of an experiment, $f_\parallel(t)$ and $f_\perp(t)$ curves cannot simply be collected for equal time periods, but must be normalized after data collection. Although this can be done by comparing the total counts in the $f_\parallel(t)$ and $f_\perp(t)$ decay curves over short time intervals on the nanosecond apparatus (Yguerabide et al., 1970), the steady-state fluorescence determination of this normalization ratio $(\bar{F}_\parallel/\bar{F}_\perp)$[2] is more reproducible and is the method which we employed (Dale and Eisinger, 1975). Steady-state fluorescence measurements of $\bar{F}_\parallel/\bar{F}_\perp$ were carried out at 25 °C with an Aminco SPF-1000 corrected spectrophotofluorimeter as described in the previous paper (Holowka and Cathou, 1976). Excitation and emission light were polarized by Polacoat ultraviolet polarizing filters, and monochromator polarization effects were corrected for (Chen and Bowman, 1965). Wavelengths and spectral band widths were nominally the same as those employed in the nanosecond apparatus, and good agreement was obtained between the ratios measured by the two instruments. Normalization was accomplished by scaling $f_\parallel(t)$ and $f_\perp(t)$ to make the ratio of the areas under their curves equal to $\bar{F}_\parallel/\bar{F}_\perp$.

Fluorescence lifetime data were deconvoluted and analyzed by the method of moments (Isenberg and Dyson, 1969) with a Fortran program (C. Cantor, unpublished program), and computations were performed by an IBM 360 computer. Analysis by this program yields a best fit of the deconvoluted data in the form of one to three exponential terms:

$$S(t) = \sum_{i=1}^{3} \alpha_i e^{-1/\tau_i} \tag{2}$$

where $S(t)$ is the total (unpolarized) emission, τ_i is the fluorescence lifetime, and α_i is the relative weighting factor. The lamp profile used in the deconvolution was obtained by scattering the excitation-filtered lamp pulse directly onto the photomultiplier (no emission filter) with Ludox (Du Pont), a commercial scattering colloidal suspension. It was found that, when the raw nanosecond depolarization decay curves $f_\parallel(t)$ and $f_\perp(t)$ were deconvoluted separately and the best fits (one to three exponential terms) were used to calculate the anisotropy decay curve, it did not differ significantly from that calculated with the convoluted (raw) data at short times (0–80 ns), but usually dropped or rose sharply at longer times, indicating that the best fit of the data was not accurate enough to give meaningful results at these longer times in the decay. Consequently, since we found that the anisotropy decay at short times (0–80 ns) was not measurably affected by convolution of the data with the lamp pulse, the raw data were used in all calculations.

Analysis of the Nanosecond Depolarization Decay Curves. In the cases where a rigid prolate ellipsoid might be considered a reasonable approximation to the hydrodynamic shape of the macromolecule, namely for the proteolytic fragments, the normalized three-exponential expression of Tao (1969) was employed in an attempt to fit the decay data to a simple model system:

$$A(t)/A_0 = \sum_{i=1}^{3} f_i e^{-(t/\phi_0)\Omega_i} \tag{3}$$

where A_0 is the initial anisotropy, ϕ_0 is the rotational correlation time of a rigid sphere with the same volume, f_i is dependent on the angle θ between the emission transition dipole and the major axis of the prolate ellipsoid, and Ω_i is dependent on γ, the axial ratio of the ellipsoid, as defined by Yguerabide et al. (1970). In the case of random orientation of the transition dipole, eq 3 simplifies to:

$$A(t)/A_0 = \frac{2}{3} e^{-(t/\phi_0)\Omega_2} + \frac{1}{3} e^{-(t/\phi_0)\Omega_3} \tag{4}$$

where Ω_2 and Ω_3 are functions of the prolate axial ratio as described by Yguerabide et al. (1970). ϕ_0 can be calculated from the following expression:

$$\phi_0 = \eta M(\bar{v} + h)/RT \tag{5}$$

where η is the viscosity of the solution, M is the molecular weight of the molecule, $\bar{v}$ is the partial specific volume, h is the hydration, R is the gas constant, and T is the temperature (Yguerabide, 1972). For a given value of ϕ_0, the normalized anisotropy decay is dependent only on θ and γ which can be determined by independent means; then ϕ_0 and hence the effective hydration of the molecule can be found.

In cases of molecules with more complex shapes and/or which may be flexible, model ellipsoid calculations are of little help except to rule out certain possibilities. As the simplest interpretation for a curved log $A(t)$ decay, two major modes of Brownian rotation were assumed to account for the decay, and the data were fit to the sum of two exponential terms by a nonlinear, least-squares analysis (Marquardt, 1963) weighted with $1/A(t)$ and using 300–400 data points (channels) for each curve (Massachusetts Institute of Technology

[2] $\bar{F} = \int_0^\infty F(t)dt$, where $F(t)$ is the deconvoluted fluorescence.

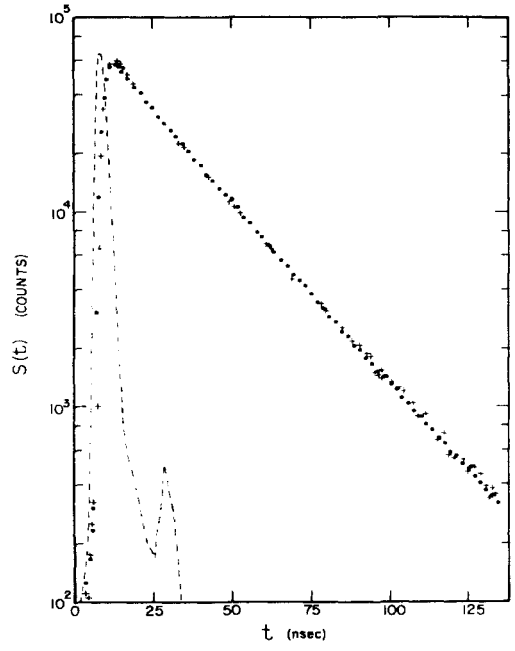

FIGURE 1: Fluorescence emission decay kinetics of DNS-lysine in the equine anti-DNS IgM combining site. (●) Reconvoluted best fit (two exponentials) from the method of moments analysis; (+) convoluted (raw) data points which indicate the largest deviations of the best fit analysis from the actual decay curve; (- - -) lamp profile. Excitation was at 340 nm and emission was measured at 500 nm. See Table I for lifetime values.

Subroutine LSMARQ, IBM Applications Program 84). The form of the equation employed was

$$A(t) = A_0(f_S e^{-t/\phi_S} + f_L e^{-t/\phi_L}) \quad (6)$$

where ϕ_S and ϕ_L represent the short and long rotational correlation times which together describe the time-dependent depolarization, and f_S and f_L are their respective preexponential terms (Yguerabide et al., 1970).[3] If the reporter fluorophore is randomly oriented on a segment which experiences rotational mobility independent of the whole macromolecular rotation, then ϕ_S is a measure of the rate of rotation of the segment, and f_S is a measure of the total angle traversed by the segment, relative to that of the macromolecule, during the time course examined (Weber, 1952a; Yguerabide et al., 1970).

Other Spectroscopic Measurements. The steady-state fluorescence polarization was measured at 25 °C as described above in the case of the determination of the normalization ratio, and the average anisotropy ($\bar{A}$) was calculated with a formula analogous to eq 1. $\Delta\beta_{\lambda\text{-}400}$, the angle between the transition dipole associated with excitation at the wavelength and that responsible for excitation at 400 nm, was calculated according to Schlessinger et al. (1974). Circular dichroism measurements of the equine anti-DNS–DNS-lysine complex were performed on a Jasco J20A recording spectropolarimeter. A molar excess of DNS-lysine to antibody combining sites was added, and the concentration of bound DNS-lysine was estimated from the equivalence point of a fluorescence enhancement titration (Holowka and Cathou, 1976; Parker et al., 1967). Molar ellipticity, (θ), in deg cm^2 dmol^{-1} was calculated as in Rockey et al. (1972), and the absorption anisotropy factor, g_{ab}, as in Schlessinger et al. (1974).

Results

Fluorescence Decay Kinetics. In the previous paper, the steady-state fluorescence emission characteristics were examined for the DNS-lysine–anti-DNS complexes of all three IgM species (Holowka and Cathou, 1976). Although there were some distinct species differences, DNS-lysine bound in the combining sites of all three anti-DNS antibody preparations exhibited a significant blue shift in emission maximum and a quantum yield enhancement relative to that observed in aqueous solution. The fluorescence spectra of DNS-lysine bound to acid- or hapten-eluted equine anti-DNS IgM were found to be essentially the same, as were the fluorescence titration curves. As expected by comparison with the fluorescence properties of rabbit IgG DNS-lysine–anti-DNS complexes (Parker et al., 1967; Yguerabide et al., 1970; Werner et al., 1972), the fluorescence lifetimes for DNS-lysine anti-DNS IgM complexes were also in general quite long. Figure 1 shows the nanosecond decay kinetics of fluorescence emission for the acid-eluted equine DNS-lysine–anti-DNS complex, along with the reconvoluted best fit of the experimental data. A single exponential fit of τ = 22.4 ns was statistically comparable (±10% of the standard deviation) to a double exponential fit of 26.6 ns (α_1 = 0.44) and 17.8 ns (α_2 = 0.56). It is difficult to choose between these two alternatives. In the case of hapten-eluted anti-DNS, the data could be fit only with a single exponential. For both preparations, the single exponential lifetime values were essentially the same. The lifetime data for all three IgM species are summarized in Table I as well as for the equine Fabμ (papain) fragment. The excitation wavelength dependence of the emission kinetics was examined for this fragment in conjunction with a study of its effect on the nanosecond depolarization kinetics (see below). The fluorescence lifetimes for the intact equine IgM and its Fabμ fragment were almost identical. Some heterogeneity was apparent in the case of the fragment, particularly at the edges of the DNS-lysine absorption band (313 and 400 nm). In light of other evidence for combining site heterogeneity, such as curvature of the Scatchard hapten-binding plot and the slight dependence of the emission spectrum on excitation wavelength (Holowka and Cathou, 1976), it is not surprising that the lifetime values also exhibit a small degree of heterogeneity. In regard to the wavelength dependence of the rotational correlation time which will be discussed below, it should be noted here that there was no significant difference between the fluorescence lifetime analysis of the DNS-lysine–Fabμ (papain) complex at the short and long wavelength sides of the absorption band. The porcine DNS-lysine–anti-DNS IgM complex also exhibited some heterogeneity of fluorescence lifetime, as shown in Table I. Of prime importance for the depolarization studies is the fact that the longer lifetime component was relatively constant in magnitude (22.4–26.6 ns) and was the predominant emitting species for both equine and porcine anti-DNS IgM.

The nurse shark anti-DNS IgM fluorescence decay kinetics were significantly different, however. As can be seen in Table I, this DNS-lysine–antibody complex exhibited both a long lifetime component and a short lifetime component which was the predominant emitting species. The population of DNS molecules which exhibit such a short lifetime must be more

[3] In reality, the simplest equation which can be derived for the case in which a fluorophore is rotating on a segment of a macromolecule is a three exponential expression $A(t) = A_0[Xe^{-t((1/\phi_L)} + Ye^{-t(((1/\phi_L)+(2/3\phi_S))} + Ze^{-t(((1/\phi_L)+(1/6\phi_S))}]$ where X, Y, and Z are related to the angles which the absorption and emission oscillators make with the axis of rotation (Ehrenberg and Rigler, 1972). However, since the conditions of this equation, namely that the segmental rotation is tortional about a single axis and the macromolecule itself is spherical in shape, are probably not fulfilled in the case of IgM, it was not felt that the use of this equation was anymore justified in the present case than the use of eq 6.

TABLE I: Summary of Fluorescence Lifetimes of Antibody-Bound DNS-Lysine.

DNS-Lysine Complex:	Excitation Wavelength[a,b] (nm)	Lifetimes[c] α_1	τ_1 (ns)	α_2	τ_2 (ns)
Equine anti-DNS IgM (hapten eluted)	355 (54)	1.00	21.6		
Equine anti-DNS IgM (acid eluted)	340 (14)	1.00	22.4		
		Or[d]			
		0.44	26.6	0.56	17.8
Equine Fabμ (papain)	313 (12)	0.65	24.6	0.35	8.8
Equine Fabμ (papain)	340 (14)	0.85	24.0	0.15	7.8
Equine Fabμ (papain)	360 (11)	1.00	22.4		
Equine Fabμ (papain)	400 (9)	0.68	25.5	0.32	12.2
Porcine anti-DNS IgM	355 (54)	0.73	24.1	0.27	10.3
Nurse shark anti-DNS IgM	355 (54)	0.39	21.1	0.61	4.4

[a] Emission was in all cases at 500 nm (10-nm bandwidth). [b] Spectral bandwidth is given in parentheses. [c] See Methods. [d] Statistically equivalent (see text).

TABLE II: Rotational Correlation Times[a] (ϕ) of Fab and Fab'μ Fragments.

Fragment	Excitation Wavelength (nm)	Bandwidth (nm)	ϕ (ns)
Pepsin Fabμ (equine)	355	54	31.5
Papain Fabμ (equine)	355	54	32.0 ± 2[b]
Papain Fabμ (equine)	313	12	32
Papain Fabμ (equine)	360	11	35
Papain Fabμ (equine)	400	9	36
Pepsin Fabμ (porcine)	355	54	36
Pepsin Fab'μ (equine)	355	54	41.5[c]

[a] Single exponential best fit at 25 °C. Emission was measured at 500 nm. [b] Average error of four experiments. [c] Linear fit from 0 to 65 ns (see text).

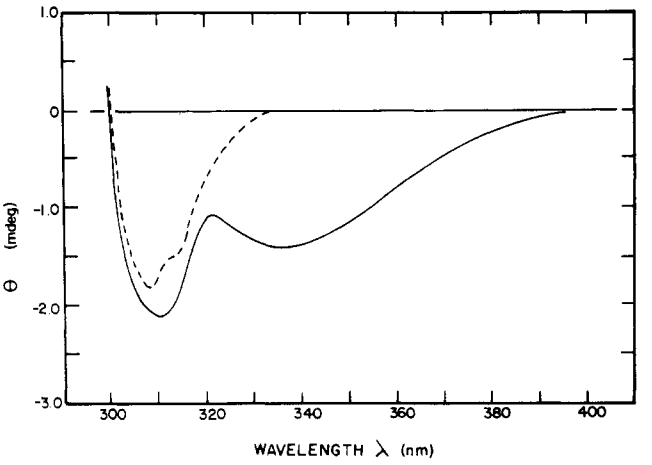

FIGURE 2: Induced circular dichroism of DNS-lysine in the equine anti-DNS antibody combining site. The ordinate is observed ellipticity. Anti-DNS antibody (90% IgM) was at a concentration of 1.5 mg/ml; cell path length was 5 cm. (- - -) Anti-DNS antibody; (—) anti-DNS antibody with a molar excess of DNS-lysine with respect to combining sites.

susceptible to nonradiative deactivation of the excited state; they may thus be more exposed to solvent and may possibly have some freedom of rotation within the combining site. It may be this population which was responsible for the very short correlation time observed in the depolarization decay (see below). The modes of rotation monitored by the short lifetime component should be weighted differently from those monitored by the longer lifetime component, but the magnitudes of ϕ measured by both components should be the same, provided that the emitting dipoles have similar or random orientations on the macromolecule. It should be stressed, however, that a long lifetime component which could monitor slower macromolecular rotations was present in the shark DNS-lysine–anti-DNS complexes.

Rigidity of Hapten Binding. The presence of a short lifetime subpopulation of DNS-lysine in shark DNS-lysine–anti-DNS complexes which might possibly have some independent rotation prompted us to investigate the rigidity of binding of DNS-lysine in the combining sites of the other species of anti-DNS IgM. It was shown by Brochon and Wahl (1972) that DNS *covalently conjugated* to IgG showed measurable rotational correlation times of 2–4 ns which were attributed to partially hindered dye rotation around covalent bonds on the macromolecule. However, for a hapten such as DNS-lysine *noncovalently bound* in an antibody combining site, it is expected that multipoint attachment to specific amino acid residues via hydrophobic and van der Waals interactions would prevent the hapten from tumbling freely in the site. In the case of acid-eluted equine anti-DNS IgM at least, this appears to be true, since the binding of DNS-lysine in the combining site induced an asymmetric environment which resulted in measurable induced circular dichroism of the lowest energy absorption band (see Figure 2). The value of the molar ellipticity [θ] at the maximum wavelength, 340 nm, is -2.5×10^3 deg cm^2 dmol^{-1}. This corresponds to an absorption anisotropy factor, g_{ab}, of -0.94×10^{-4} (Schlessinger et al., 1974). Moreover, circularly polarized luminescence has been measured for a preparation of our equine anti-DNS (90% IgM) and was found to be about the same magnitude as the circular dichroism (I. Pecht, personal communication). This shows that DNS-lysine in the excited state is also experiencing a symmetric environment when bound and thus it is unlikely that DNS-lysine is rotating independently within the combining site during the emission process. Further evidence for rigid binding is given by the rotational correlation times of the Fabμ fragments derived from equine and porcine IgM (see Table II and text below).

Nanosecond Depolarization of IgM. Figure 3 shows the nanosecond decay of emission anisotropy, $A(t)$, of DNS-lysine

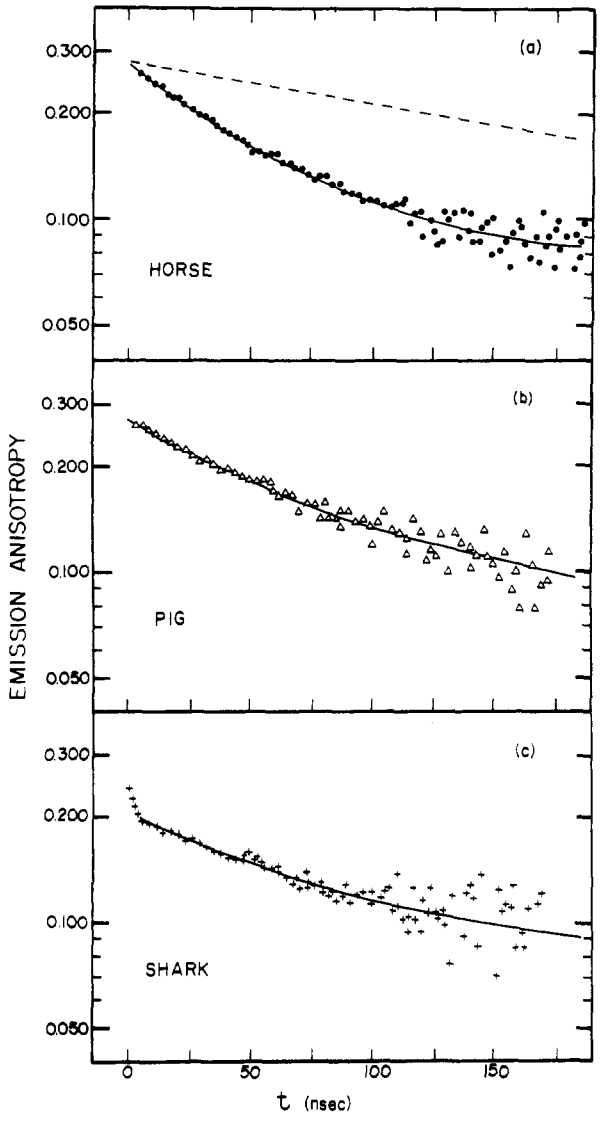

FIGURE 3: Time dependence of the emission anisotropy $[A(t)]$ of DNS-lysine in the combining site of anti-DNS IgM. (a) Equine IgM (hapten eluted); (●) representative data points; (- - -) calculated decay for a rigid, hydrated sphere with the same volume as IgM. (b) Porcine IgM; (△) representative data points. (c) Nurse shark IgM; (+) representative data points. Solid lines are the least-squares best fit of eq 6 to the observed data. Excitation was at 355 nm; emission was measured at 500 nm. See Table III for values of rotational correlation times.

bound in the anti-DNS combining sites of IgM from the three species: horse, pig, and nurse shark. The long fluorescent lifetime components which predominated for DNS-lysine bound to both equine and porcine IgM (22-27 ns) allowed statistically significant data to be obtained at times as long as 175 ns. The initial anisotropy, A_0, was taken at the peak of the lamp pulse, as reproducible data could be obtained only after this point. The plot of log $A(t)$ exhibits curvature for each species of IgM, indicating that several rotational correlation times are present. In Figure 3a, the dotted line depicts the anisotropy decay expected for the rotation of IgM as a rigid, hydrated sphere with ϕ_0 = 380 ns and A_0 = 0.280.[4] This line represents the fastest decay of anisotropy which could be expected if IgM behaved hydrodynamically as an inflexible macromolecule with DNS-lysine bound rigidly in the combining sites. For equine anti-DNS IgM, this quite clearly is not the case since at least one rotational correlation component, as estimated by the slope of a tangent to the curve at any point, is considerably less than 380 ns. Further, it can be seen that such a correlation time must be smaller than 0.95 ϕ_0 so that we are not observing the motion of a rigid but highly asymmetric particle (Tao, 1969).

As seen in Figure 3b, the plot of log $A(t)$ for porcine anti-DNS IgM exhibits curvature which is similar to that of the plot of equine IgM, as is the initial anisotropy value. This decay curve also has at least one rotational correlation component which is considerably shorter than 380 ns.

The nurse shark anti-DNS IgM depolarization decay curve (Figure 3c) consists of at least two components with correlation times shorter than 380 ns and an additional very long component. On analysis, the very fast initial decay had a value of ϕ which ranged from 3 to 13 ns, after the longer components were subtracted, and is too short to be attributed to the rotation of a rigid Fabμ-like fragment, which would be expected to have a value of ϕ of at least 20 ns. Further analysis and discussion of the nurse shark IgM decay curve will be considered below.

Nanosecond Depolarization of Fabμ. To ascertain whether the short component contributing to depolarization in Figures 3a and 3b can be correlated with the motion of Fabμ and to determine whether the DNS-lysine was indeed rigidly bound in the combining sites, proteolytic fragments of the equine IgM were prepared. The anisotropy decay for the equine Fabμ (papain) fragment prepared from the acid-eluted preparation was single exponential, with ϕ = 32 ns (Figure 5). Equine Fabμ (pepsin) yielded identical results (see Table II). These values are in agreement with the value of ϕ obtained for Fabγ (Yguerabide et al., 1970), and show that DNS-lysine Fabμ rotates as a single rigid molecule, with no shorter rotational correlation times present during the time scale examined. In this regard it may be noted that the implied flexibility at the switch peptides connecting V and C domains within the Fab segment, as suggested by the recent x-ray crystallographic studies of Colman et al. (1976) on a human myeloma IgG1 and the ESR studies by Käiväräinen et al. (1973), is not apparent on the nanosecond time scale for the Fab fragment from either IgM or IgG.

Similar results were obtained with porcine Fab; the value of the single rotational correlation time is also given in Table II. In this case ϕ was longer than that of equine Fabμ when the same excitation filter was employed; this may be attributable to a slightly higher molecular weight for porcine Fabμ (Zikán and Miler, 1974). Thus it can be concluded that the fluorophore exhibits no independent rotation of its own in either equine or porcine IgM, and the curvature seen in Figures 3a, 3b, and 4 must be the result of segmental motion of the macromolecule itself.

Effect of Acid Exposure on Equine IgM. In our initial studies on equine anti-DNS IgM, we employed the acid-eluted antibody, and, as shown in Figure 4, we were surprised to find that the log $A(t)$ plot for this preparation exhibited even more curvature than that for the hapten-eluted IgM. It is obvious that a significant increase in the rotational freedom of the bound DNS-lysine had taken place on exposure of the antibody to 1 M acetic acid, although the CD results and the anisotropy decay of the Fabμ fragments indicated that the hapten was still rigidly bound in the combining sites.

Nanosecond Depolarization of Equine (Fab′)$_2\mu$. Figure 5 shows the anisotropy decay for the equine (Fab′)$_2\mu$ fragment

[4] ϕ_0 was calculated according to eq 5, assuming a molecule weight of 900 000 and $\bar{v}$ = 0.715 ml/g (Dorrington and Tanford, 1970); a minimum hydration was estimated to be 0.45 g of H_2O/g of protein.

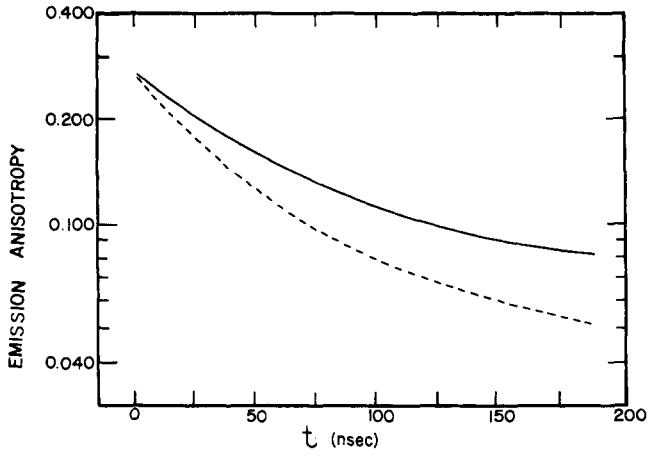

FIGURE 4: Comparison of the emission anisotropy decay of acid-eluted equine IgM with that of hapten-eluted equine IgM. (—) Best fit of eq 6 to observed $A(t)$ for DNS-lysine bound to hapten-eluted anti-DNS IgM; (- - -) best fit of eq 6 to observed $A(t)$ for DNS-lysine bound to *acid-eluted* anti-DNS IgM.

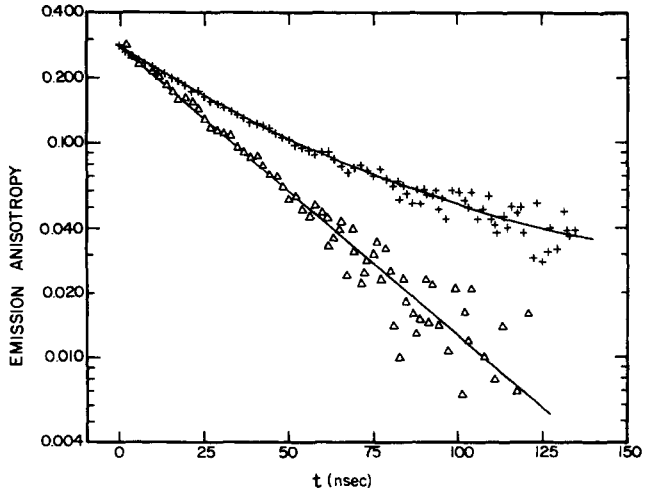

FIGURE 5: Time dependence of the emission anisotropy of DNS-lysine bound to equine $(Fab')_2\mu$ (+) and Fabμ (papain) (Δ) fragments. Solid lines represent the least-squares best fit of the observed data. The excitation wavelength was 355 nm and the emission wavelength was 500 nm.

prepared from acid-eluted anti-DNS IgM. Although the log $A(t)$ plot in this case is somewhat curved, it is not immediately obvious whether segmental flexibility or asymmetry is the major cause of depolarization. The presence of the Cμ2 domain in this fragment (Shimizu et al., 1974) makes each Fab'μ segment three domains long instead of two as in Fabγ (Dorrington and Tanford, 1970). Since there appears to be very little noncovalent interaction between the Cμ2 domains in this fragment (Holowka and Cathou, 1976), one possible conformation might be a long rigid ellipsoid in which the Fab'μ segments are aligned end-to-end connected by the μ–μ interchain disulfide bonds at their C-terminal ends. Because of the large difference in Ω_i values (eq 3) expected for such an ellipsoid (axial ratio ca. 6:1), the log $A(t)$ plot would exhibit significant curvature in the time range we are examining (Tao, 1969; Figure 7). Calculation of the expected anisotropy curve for an equivalent ellipsoid would help to resolve this question.

Model Ellipsoid Calculations. In order to determine whether the log $A(t)$ decay curve of $(Fab')_2\mu$ can be attributed to that of a rigid ellipsoid, a number of parameters must first be known, i.e., ϕ_0, f, and Ω_i (see eq 3 and 4). To calculate ϕ_0, from eq 5, one needs values of the hydration (h), the molecular weight, and the partial specific volume. Of these parameters, only the value of h is unknown; it is difficult to determine h directly, but we can get an estimate of it from the hydration of the Fab fragment, a rigid ellipsoid with known molecular dimensions (by analogy to Fabγ). Since this latter fragment is known to approximate a prolate ellipsoid with an axial ratio of 2:1 (Poljak et al., 1973; Pilz et al., 1975), if we knew the orientation of the transition dipole moment of DNS-lysine on the macromolecule (e.g., preferential or random), we could calculate h from the observed value of ϕ.

Although the observed heterogeneity of combining sites in which DNS-lysine is bound would make preferential orientation of this hapten unlikely, we felt it was necessary to try to establish this experimentally. Witholt and Brand (1970) have introduced a method based on depolarization of fluorescence at different excitation wavelengths which allows one to distinguish between random and nonrandom orientation of a multioscillator fluorophore bound rigidly to a prolate ellipsoid. For DNS-lysine in the Fabμ (papain) combining site, the anisotropy, $\bar{A}$, was found to increase continually across the lowest energy absorption band, reaching a maximum value of 0.180 at 400 nm. This type of behavior can be attributed to the presence of two or more closely spaced transition dipoles which are probably at slightly different angles with respect to each other (Li et al., 1975). The angle between the transition dipole associated with excitation at 313 nm and excitation at 400 nm, $\Delta\beta_{313-400}$, was calculated to be 4.5° (see Methods). This angle is small compared with that calculated for other aminonaphthalenes, such as 1-anilino-8-naphthalenesulfonate ($\Delta\beta_{340-420}$ = 18.5°, calculated from Anderson and Weber, 1969), but angles of similar magnitudes are large enough to show measurable differences between Perrin plots for an equatorially oriented fluorophore on bovine serum albumin (see Figure 10 of Witholt and Brand, 1970).

When the emission anistropy decay was determined for the Fabμ (papain) fragment by excitation at 313 nm, the log $A(t)$ plot was straight and the rotational correlation time was 32 ns, a value identical with that observed for excitation with the broad-band filter (λ_{max} 355 nm). These results suggested that the Fabμ (papain) fragment was behaving as a rigid prolate ellipsoid of the same dimensions as the Fabγ fragment with a randomly oriented fluorophore in the combining site. However, when excitation was at 360 or 400 nm, the depolarization behavior was different: Although the anisotropy decay was still single exponential, the rotational correlation time was longer, with ϕ = 35 ns at 360 nm and ϕ = 36 ns at 400 nm. These results are summarized in Table II. It is unlikely that these differences can be attributed to significant size heterogeneity of the Fabμ (papain) fragment since the DNS-lysine-binding fragment is eluted as a single symmetrical peak on Sephadex G-200 (Holowka and Cathou, 1976). It was therefore concluded that some preferred, although unknown, orientation of the DNS-lysine in the Fabμ (papain) combining sites might be present, but that this behavior was exhibited only by those molecules of DNS-lysine which were preferentially excited on the long wavelength side of the absorption band.

To simplify the analysis, let us examine the range of values of h which can be calculated for the extreme cases of dipole orientation as well as for random orientation. Then a comparison of these values with literature values should allow us to choose a reasonable approximate value of h. If we assume the case in which the absorption dipole is oriented perpendicular to the major axis of the ellipsoid (θ = 90°), then the best fit of the normalized anisotropy decay plot using eq 3 (not

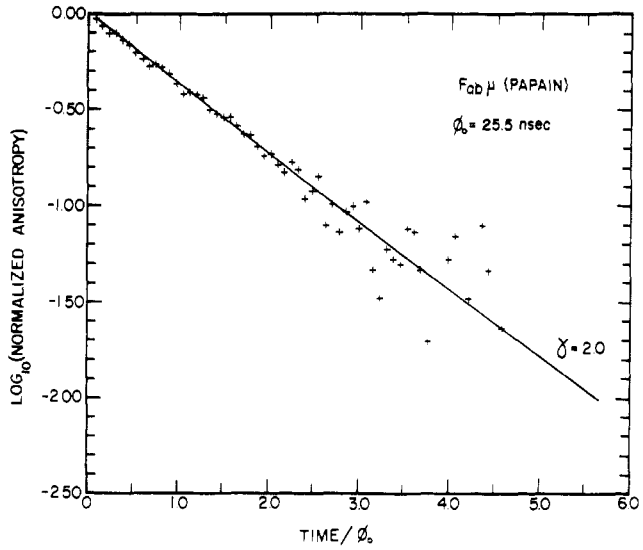

FIGURE 6: Comparison of observed and calculated normalized anisotropy plots for equine Fabμ (papain). (+) Observed data, normalized with ϕ_0 = 25.5 ns and A_0 = 0.30; (—) normalized anisotropy decay curve for a rigid prolate ellipsoid of axial ratio 2:1 in which the fluorophore is randomly oriented relative to the ellipsoid axes. λ_{ex} = 355 nm; λ_{em} = 500 nm.

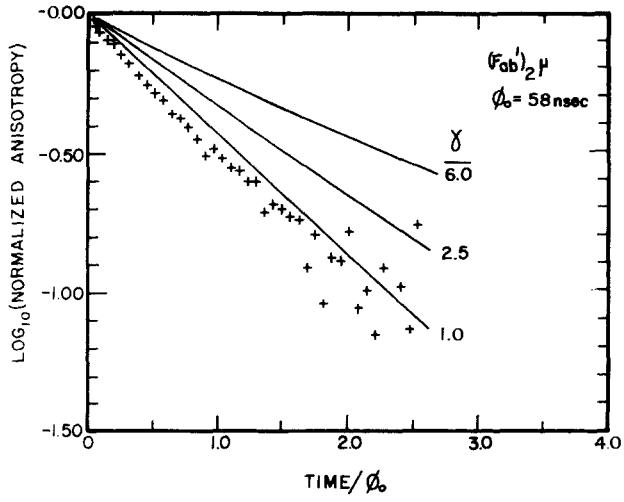

FIGURE 7: Comparison of observed and calculated normalized anisotropy plots for equine (Fab')$_2\mu$. (+) Observed data, normalized using ϕ_0 = 58 ns and A_0 = 0.285; (—) normalized anisotropy decay curves for rigid prolate ellipsoids of axial ratio 1.0, 2.5, and 6.0:1 assuming random orientation of the fluorophore relative to the ellipsoid axes. λ_{ex} = 355 nm; λ_{em} = 500 nm.

shown) yields a minimum value of ϕ_0 = 28.4 ns. For a molecular weight of 50 000 and $\bar{v}$ = 0.725[5] (Chen et al., 1969), h = 0.86 g of H_2O/g of protein. This is an unreasonably high value even when the contribution of loosely associated water molecules is taken into consideration (Kunitz and Kauzman, 1974). By comparison, a value of 0.36 was found for the Fabγ fragment from low angle x-ray scattering (Pilz et al., 1975). For the other extreme case, namely orientation of the dipole along the major axis of the ellipsoid (θ = 0°), the expression derived by Tao (eq 3) becomes single exponential:

$$A(t) = A_0 e^{-(t/\phi_0)\Omega_i} \quad (7)$$

Using the value of ϕ = 36 ns (λ_{ex} 400 nm), since this is the rotational correlation time for the most oriented molecules of DNS-lysine, and taking Ω_i from Table II of Tao (1969), ϕ_0 = $\phi\Omega_i$ and the hydration in this case is calculated to be 0.67 g of H_2O/g of protein. This value is still higher than expected but is more reasonable than that calculated for the first case. Finally, the random orientation case may still apply for excitation between about 310 and 360 nm. Figure 6 shows the normalized plot for Fabμ (papain) assuming random orientation of the DNS-lysine emission dipole, with excitation at 355 nm, and it is clear that the model prolate ellipsoid provides a reasonable description of the anisotropy decay in the time scale examined. From this fit, ϕ_0 = 25.5 ns, and h is calculated to be 0.69 g of H_2O/g of protein in agreement with the value obtained assuming θ = 0°.

Thus, regardless of whether preferred or random orientation is assumed for the binding of DNS-lysine to equine Fabμ (papain) (eliminating the first case as unreasonable), the same value for h is obtained.

If this value of 0.68 g of H_2O/g of protein is then used to calculate ϕ_0 for (Fab')$_2\mu$, assuming M = 115 000 and v = 0.715 (Metzger, 1970), the normalized anisotropy decay curves for different axial ratios can be plotted and compared with the actual decay, as shown in Figure 7. As for the case with Fabμ, the random orientation model was assumed to be the best approximation for λ_{ex} 355 nm. For the calculated value of ϕ_0 = 58 ns, the log $A(t)/A_0$ decay is faster than that expected for even the most compact model, thus indicating that some segmental flexibility must exist at this level of structure. Since it has been shown that the Cμ2 domains do not interact sufficiently to hold the Fab'μ segments together noncovalently (Holowka and Cathou, 1976), it follows then that the regions of flexibility in the (Fab')$_2\mu$ can be near either the Cμ1–Cμ2 domain junction, or at a site NH_2 terminal to the inter-μ chain disulfide, or both.

Nanosecond Depolarization of Equine Fab'μ. In an attempt to elucidate the site(s) of flexibility in the (Fab')$_2\mu$ fragment, we analyzed the anisotropy decay of the Fab'μ fragment prepared by reduction and alkylation of (Fab')$_2\mu$. If the Fab'μ fragment is rigid, i.e., if no flexibility is present between the Cμ1 and Cμ2 domains, then we would expect the normalized anisotropy plot to correspond to that of a rigid ellipsoid with an axial ratio of approximately 3:1. On the other hand, the presence of a flexible hinge between the Cμ1 and Cμ2 domains would result in a more complex decay curve which would probably be closer to that of an ellipsoid with an axial ratio of 2:1. The normalized plot of a log $A(t)/A_0$ vs. t/ϕ_0 is shown in Figure 8, along with calculated curves for which random orientation of the emission dipole and ϕ_0 = 29 ns were assumed. The experimental data are significantly different from those obtained for the Fabμ fragment, as might be expected due to the presence of the additional domain (Cμ2), and appear to fall between the plots calculated for prolate ellipsoids with axial ratios of 2.0 and 3.0. In two separate preparations examined, the log $A(t)$ plot was essentially linear in the time range 0 to 65 ns, with values for ϕ of 41 and 42 ns, respectively. Unfortunately, the quality of the data does not permit us to determine whether flexibility exists at the junction of the Cμl and Cμ2 domains in this fragment.

Calculation of Rotational Correlation Times of IgM and (Fab')$_2\mu$. A weighted, nonlinear, least-squares analysis was applied to the depolarization curves of IgM and the (Fab')$_2\mu$ fragment; the results are summarized in Table III. With the exception of the time dependent anisotropy of nurse shark IgM, the two exponential expression of eq 6 gave a reasonable fit to the experimental data (Figures 3a and 3b for equine and por-

[5] $\bar{v}$ for Fabμ is larger than that for whole IgM because of the lower carbohydrate content of the former.

TABLE III: Rotational Correlation Times of IgM and $(Fab')_2\mu$.[a]

Immunoglobulin	A_0	t_{max} (ns)[b]	f_S	ϕ_S (ns)	f_L	ϕ_L (ns)
Equine $(Fab')_2\mu$[c]	0.280	135	0.79	38	0.21	211
Equine IgM, acid eluted	0.274	175	0.69	40	0.31	355
Equine IgM, hapten eluted	0.274	170	0.71	61	0.29	>1000
Porcine IgM	0.274	175	0.57	69	0.43	568
Nurse shark IgM[d]	0.242	160	0.63	93	0.37	>1000

[a] Best fits from nonlinear, least-squares analysis using eq 6. [b] Longest time from which $A(t)$ data points were used in analysis. [c] Prepared from acid-eluted IgM. [d] Initial fast decay component not included in analysis.

cine IgM, and Figure 5 for the equine $(Fab')_2\mu$ fragment). In the case of nurse shark IgM, the analysis was applied to the curve after the decay of the initial fast component (Figure 3c).

It is immediately evident from Table III that both acid-eluted equine IgM and the $(Fab')_2\mu$ fragment derived from it exhibit a short rotational correlation time (ϕ_S) of the same magnitude. This component is the larger contributor to the depolarization in both cases (f_s = 0.69–0.79), and is significantly larger than the value of ϕ of a freely tumbling Fabμ fragment (32 ns) determined under similar conditions. However, it is closer to the values estimated for the Fab'μ fragment (41–42 ns). The value of ϕ_S of the hapten eluted equine IgM is significantly longer than that of acid-eluted IgM, but is still the predominant depolarization component.

ϕ_L of $(Fab')_2\mu$, although subject to larger errors than ϕ_S, probably represents the Brownian rotation of the entire fragment, and its magnitude suggests a fairly extended conformation. ϕ_L of hapten-eluted equine IgM is too long to be measured accurately, and probably is due to the rotation of the entire macromolecule. The value of ϕ_L for the acid-eluted equine IgM is considerably shorter, but probably represents only an approach to the value of a longer rotational correlation time, since data fit only for $0 < t < 150$ ns resulted in a much shorter value for ϕ_L, i.e., 173 ns, *while the value of ϕ_S remained essentially the same in both cases.*

Porcine IgM exhibits a value of ϕ_S which is only slightly longer than that of hapten-eluted equine IgM, and f_s is somewhat smaller. However, the value of ϕ_L is definitely within the limits of measurement, and unlike the value of ϕ_L of acid-eluted equine IgM, does not change significantly when the analysis is carried out for $0 < t < 135$ ns instead of for $0 < t < 175$ ns.

In an attempt to ascertain the physical significance of the value of ϕ_L of porcine IgM (568 ns), the $(Fc)_5\mu$ fragment was prepared and conjugated with DNS. The DNS-$(Fc)_5\mu$ gave a single symmetrical schlieren peak on analytical ultracentrifugation, with an $s_{20,w}$ value of 10.6S at 0.40 mg/ml, and appeared to have about 10 mol of DNS per mol or $(Fc)_5\mu$ [molecular weight 320 000 (Zikăn and Miler, 1974)]. There were apparently no Fab'μ arms remaining on the $(Fc)_5\mu$ fragment since DNS-lysine could not be titrated into the unconjugated fragment. A two-exponential fit of the fluorescence decay curve gave values of $\alpha_1 = 0.30$, $\tau_1 = 17.9$ ns and $\alpha_2 = 0.70$, $\tau_2 = 6.7$ ns, so that a long lifetime component capable of detecting a rotational correlation time of at least 600 ns was present (Wahl et al., 1971). The log $A(t)$ plot exhibited an initial rapid decay which probably can be attributed to partially hindered dye rotation, but then straightened out after about 12 ns and became essentially horizontal with a value of ϕ greater than 800 ns. This value is quite surprising since it is larger than ϕ_L for intact porcine IgM, and because the calculated value of ϕ_0 of the *unhydrated* $(Fc)_5\mu$ fragment is about 80 ns; the fragment must thus be highly hydrated and extremely asymmetric or some aggregates not detected in the ultracentrifugation may have been present. We have no explanation for these results at present.

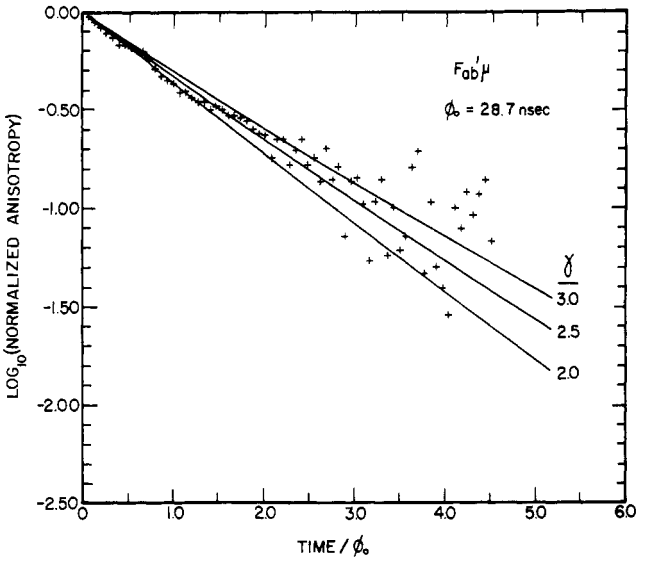

FIGURE 8: Comparison of observed and calculated normalized anisotropy plots for equine Fab'μ. (+) Observed data normalized using ϕ_0 = 28.7 ns and A_0 = 0.280; the solid lines represent the normalized anisotropy decay curves for rigid prolate ellipsoids of axial ratio, 2.0:1, 2.5:1, and 3.0:1 assuming random orientation of the fluorophore relative in the ellipsoid axes. λ_{ex} = 355 nm; λ_{em} = 500 nm.

When the anisotropy decay of nurse shark IgM was analyzed at times after the initial fast depolarizaton was essentially over, it was composed of a very long ϕ_L, as observed with hapten-eluted equine IgM, and an intermediate value of ϕ_S which was significantly longer than that seen for either porcine or equine IgM. The presence of this latter component indicates that at least some segmental flexibility is also present in this phylogenetically distant IgM species.

Discussion

IgM is Flexible. The results of the nanosecond depolarization studies of equine IgM and its fragments clearly demonstrate that segmental flexibility exists in this molecule on a nanosecond timescale. The curvature of the log $A(t)$ plots of whole equine IgM (hapten and acid eluted) cannot be attributed to free rotation of the hapten, DNS-lysine, as the induced circular dichroism and the single exponential decay of $A(t)$ for the Fabμ fragment indicate that the hapten is held rigidly in the combining site during the timescale of these experiments. Free rotation of the fluorophore would also result

in a much shorter value of ϕ_S than is experimentally observed (Brochon and Wahl, 1972). Schlessinger et al. (1974) have found that the excited state circularly polarized luminescence of DNS-lysine bound to rabbit IgG anti-DNS antibodies is significantly greater than the ground-state circular dichroism. This observation suggests that the interaction of the excited state of DNS-lysine with the combining site is different than that of the ground state. Such a change in interaction, if it involved rotation of the hapten in the site, would have to be rapid relative to the emission process, and might in part account for the lower than maximal value of A_0 which we observe in anti-DNS IgM (0.28 vs. 0.40). Secondly, the depolarization behavior cannot be ascribed to a high degree of asymmetry since the observed values of ϕ_s are much shorter than 0.95 ϕ_0.

The Nature of Segmental Flexibility in IgM. The degree of flexibility in equine IgM increases upon exposure of the antibody to acid pH since the values of ϕ_S and ϕ_L both decrease. When the anisotropy decay curves of the acid-eluted equine IgM and the $(Fab')_2\mu$ fragment prepared from it were analyzed by means of a two-exponential equation, the values of ϕ_S were found to be similar (38–40 ns). Since the free Fabμ fragment behaves as a rigid entity, then either the Fabμ or somewhat larger Fab'μ fragment (which contains the Cμ2 domain) is the most likely candidate for the rotational subunit and must therefore have some freedom of rotation within the acid-eluted IgM molecule.

The simplest explanation for these results is that the entire Fab'μ segment has freedom of rotation at a site amino-terminal to the first interchain disulfide bridge in both the acid-eluted IgM and the $(Fab')_2\mu$ fragment. This possibility is supported by the similar values of ϕ_S of IgM, $(Fab')_2\mu$, and of the isolated Fab'μ fragment. In order for the Fab'μ segment to exhibit substantial freedom of rotation, the interactions between the Cμ2 domains on adjacent heavy chains must be weak and, in fact, lack of significant interaction is supported by the observation that, upon reduction and alkylation of the $(Fab')_2\mu$ fragment, the resulting Fab'μ fragments do not remain associated (Holowka and Cathou, 1976).

It is still possible that an additional site of flexibility between Fabμ and the Cμ2 domain is present. However it appears unlikely that motion of *only* Fabμ could account entirely for the observed results. If this were the case, then the rate of rotation of Fab in IgM must be slower than the rate of rotation of Fab in IgG, even though both isolated Fab fragments exhibit identical rotational correlation times (e.g., 32–33 ns) (Yguerabide et al., 1970; Holowka, 1975). This situation is hard to reconcile with the larger preexponential factor, f_s, found for IgM (f_s = 0.69) than for IgG (f_s = 0.44) which indicates that segmental motion in IgM accounts for a greater portion of the depolarization. Since f_s has been correlated with the angle through which a segment can move, the Fabμ would thus have to move more slowly through a larger angle during a similar time scale (Weber, 1952a; Yguerabide et al., 1970). While this possibility cannot be ruled out, it appears unlikely.

In the case of native (hapten eluted) equine IgM, the value of ϕ_S is longer than that seen for isolated Fabμ or Fab'μ fragments (see Table III). This strongly suggests that *the Cμ2 domains in the native IgM are associated with each other* to a sufficient degree to hinder the rotational freedom of Fab'μ which is observed after acid exposure. This possibility is supported by other observations. Although $(Fab')_2\mu$ and Fcμ from native human IgM essentially dissociate into their respective half-molecules upon reduction and alkylation (Shimizu et al., 1974; Hester et al., 1975), the half-subunits of reduced and alkylated IgMs remain associated ($K_0 \sim 4 \times 10^5$ M^{-1}; Solheim and Harboe, 1972). This indicates that both of these regions probably contribute to the overall association, although the individual interactions between adjacent Cμ2 domains and in Fc may be weak.

If one assumes that the chain folding in the Cμ2 domains is similar to that present in the Cγ1 and C_L domains of IgG, the surface residues of the analogous pleated sheet regions appear to be similar in terms of hydrophobicity and potential for domain interaction *with the exception of one or two residues in Cμ2 which are charged* and which could interfere with Cμ2–Cμ2 association (E. Padlan, personal communication).

Weak interactions between the Cμ2 domains may be particularly sensitive to external perturbing agents which lead to irreversible conformational changes. The differential effects of heat (Plaut and Tomasi, 1970) and urea (Shimizu et al., 1974) on the trypsin digestion of human IgM can be accounted for by an irreversible exposure of trypsin-sensitive sites in the Cμ2 domain following these treatments. Equine IgM antipneumococcal antibodies have been shown to be especially sensitive to heat treatment with regards to their complement-fixing ability (Deutsch and Amiraian, 1968), and similar correlations of heat and urea treatment with the destruction of complement fixation by rabbit IgM have been reported (Cunniff et al., 1968). Recently, it has been found that exposure of rabbit IgM to acid pH (pH <4) also destroyed complement fixation, even though antigen binding was not affected (Stollar et al., 1976). Thus, it is tempting to speculate that Cμ2–Cμ2 domain interaction may be involved in the activation of binding of the first component of complement (C1q) by antigen. The proper interaction of these domains, governed by a particular spacing of the antigenic determinants in the antigen–IgM complex may be the trigger which exposes the C1q binding sites on the $(Fc)_5\mu$ region. Acid treatment of IgM, which prevents the proper antigen-induced conformation necessary for tight C1q binding, would do so by destroying the Cμ2–Cμ2 noncovalent interaction. Recent evidence that monovalent antigen is sufficient to trigger complement activation in rabbit IgM (Brown and Koshland, 1975) is difficult to explain without invoking an allosteric mechanism (Metzger, 1974), but a conformationally sensitive Cμ2–Cμ2 interaction might make it possible to transmit a signal from the Fab to the $(Fc)_5\mu$ without significantly altering the tertiary structure of the individual domains. Such a mechanism might also operate in B-cell triggering when the antigen binds to the IgMs receptor. The role of conformational changes still remains to be assessed. It should be noted, however, that acid treatment also appears to make the $(Fc)_5\mu$ more susceptible to enzymatic digestion (Holowka and Cathou, 1976), so that complement-fixation-sensitive alterations may be occurring in that region as well.

Physical Significance of ϕ_S of Native IgM. It is more difficult to interpret the actual physical significance of the short rotational correlation times obtained for native equine IgM and porcine IgM. The values of ϕ_S are of similar magnitude (60–69 ns) and suggest a more hindered Fabμ or Fab'μ rotation than is present in the acid-eluted equine IgM. A more precise description of the nature of such motion does not appear warranted at present. Perhaps a more reasonable, albeit more complex, interpretation is that the values of ϕ_s seen in the native equine and porcine IgM really represent an average of several values of ϕ_i, and hence several modes of motion, such as the rotation of Fabμ or Fab'μ *and* of the entire $(Fab')_2\mu$. The latter type of motion would be expected to exhibit a rotational correlation time in the range of 80 to 135 ns when the Cμ2 domains are associated. If one assumes average values of ϕ_i

of 35 and 105 ns for the rotations of Fabμ (or Fab'μ) and (Fab')2μ, respectively, a harmonic average in which the latter component contributes twice as much as the former would yield a mean rotational correlation time of roughly the same magnitude as ϕ_S obtained for native equine and porcine IgM. These two basic modes of motion are illustrated in Figure 9. Note that the bending of $(Fab')_{2}\mu$ may take place on either side of the μ–μ interchain disulfide bond, a feature which has been recently demonstrated for the hinge region of IgG by the x-ray crystallographic studies of Colman et al. (1976). These two basic modes of motion, along with the rotation of the entire IgM, are sufficient to account for all of the nanosecond depolarization data. They are also compatible with the electron micrographs of IgM which show stellate structures with varying orientations of the Fab segments, and "staple" configurations when IgM is antigen bound.

The nurse shark anti-DNS IgM depolarization is even more complex than that of the horse and pig IgM. The very fast initial depolarization component is too short to be attributed to the rotation of an Fab-like fragment. It most likely is due to some independent or partially hindered rotation of DNS-lysine within the combining site and is probably associated with the short lifetime population of DNS-lysine. With the exception of this very short component, there does not seem to be any component of less than 80 ns which can be attributed to macromolecular rotation. With anti-DNS IgM from two different nurse sharks, the value of ϕ_S ranged from 88 to 117 ns even when the analysis only included data for $0 < t < 125$ ns instead of to 175 ns. This result shows that there is no contribution from an Fab-like rotation since these values of ϕ_S are closer to the value expected for rotation of a fragment the size of $(Fab')_{2}\mu$. The Cμ2 domains in shark IgM may be more strongly associated (and possible more compact) than the analogous domains in IgM of mammalian origin. Papain or trypsin digestion of shark IgMs yields only $(Fab')_2$ and no Fab; however, after reduction of the IgMs, the susceptible bond(s) becomes exposed and Fab can be obtained (Klapper et al., 1971). Our results are in agreement with the conclusions of Zagyansky and Ivannikova (1974) who employed steady-state fluorescence polarization to examine DNS-conjugated shark IgM, and who concluded that this immunoglobulin was less flexible than those of the higher vertebrates. The steady-state results, however, did not give any indication as to the nature of the flexible segments. In this regard, it is also of interest that our steady-state polarization studies did not detect the difference between hapten- and acid-eluted equine IgM, and the higher value of ϕ obtained for porcine IgM was not considered outside the experimental error of the measurements (Holowka, 1975; Cathou et al., 1974).

Physical Significance of ϕ_L. For hapten-eluted equine IgM, the component with a long rotational correlation time appears to approach a large value which is probably due to the rotation of the whole molecule. This correlation time could probably be measured with a longer lifetime fluorophore such as pyrenebutyrate in an anti-pyrene combining site. The feasibility of this approach has been tested with an anti-pyrene IgG antibody (Lovejoy et al., 1975) and studies on equine anti-pyrene IgM are currently underway. For the porcine IgM, the value of ϕ_L is shorter, i.e., about 570 ns, even at the longest times measured, and there is no apparent flattening of the anisotropy decay curve at times as long as 175 ns. It is difficult to interpret the physical significance of this rotational correlation time since studies on the porcine $(Fc)_{5}\mu$ fragment indicated that the latter has a significantly longer value of ϕ_L than 600 ns. Although contributions to this extremely long ϕ_L from

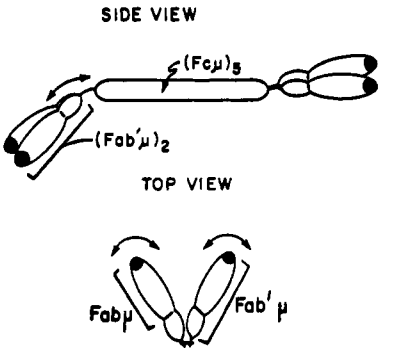

FIGURE 9: Modes of flexibility of IgM. Two possible motions, consistent with the depolarization data, are illustrated. For simplicity, only two of the five $(Fab')_{2}\mu$ regions are shown in the side view (adapted from Cathou and Holowka, 1975).

small quantities of $(Fc)_{5}\mu$ aggregates cannot be completely ruled out, it was found that reduction and alkylation of $(Fc)_{5}\mu$ resulted in a marked decrease in the value of ϕ_L as expected (unpublished observations). Actually, the high frictional ratio of $(Fc)_{5}\mu$ ($f/f_0 = 1.95$) which can be calculated from the literature values for $s_{20,w}{}^0$, and $\bar{v}$ (Plaut and Tomasi, 1970) and the molecular weight (Putnam et al., 1973) indicates that the axial ratio could be as high as 10:1 if one assumes a hydration of 0.67 g/g protein (Edsall and Mehl, 1943). The expected value of ϕ for such an oblate ellipsoid would be about 800 ns. Also, the expected symmetrical disks have not always been seen when human $(Fc)_{5}\mu$ has been examined under the electron microscope (Svehag et al., 1969; Metzger, 1974).

It is also somewhat puzzling that the value of ϕ_L of porcine IgM is smaller than that of native equine IgM. This difference may be due to the use of somewhat different purification procedures for the two antibodies. The horse anti-DNS was eluted from immunoadsorbent with hapten, whereas the porcine anti-DNS was eluted with 0.2 M acetic acid and immediately neutralized (F. Franěk, personal communication).

Conclusions

Of most significance in these findings is that IgM from both mammalian species studied, as well as from the immunologically primitive nurse shark, clearly exhibits some segmental motion, thus implicating such motion as a fundamental requirement for the function of this immunoglobulin class. It is likely that such flexibility would have advantages in the formation of antigen–antibody complexes. Although the entropy factor is minimized during the formation of multisite antigen–antibody complexes when the antibody combining sites are as close together as possible (Crothers and Metzger, 1972), flexibility should not decrease such holding power as long as these minimal site-to-site distances are attainable. On the other hand, the capturing power of a multivalent antibody such as IgM should be enhanced by flexibility with respect to the angular orientation factor and also the minimum antigenic site density which is required (Crothers and Metzger, 1972). It is not immediately obvious, however, why the *rate* of segmental rotation should be as rapid as it is. Since the dissociation rate for a monovalent antigen–antibody interaction is maximally about 10^3 to 10^4 s^{-1} (Froese and Sehon, 1965), one would anticipate that segmental rotation in the microsecond rather than nanosecond time range would be sufficient to enhance the multivalent avidity effect.

It is more likely that the requirement for segmental flexibility extends beyond the binding enhancement effect. The correlation between the ability of IgM to fix complement and

the need to maintain some control over the degree of flexibility, which the effects of acid exposure suggest, is being examined further as it may be the key to the understanding of the conformationally subtle transfer of information from the combining site to a physically distant effector site in the IgM antibody molecule.

References

Anderson, S. R., and Weber, G. (1969), *Biochemistry 5,* 1893.

Beale, D. (1974), *FEBS Lett. 44,* 236.

Brochon, J. C., and Wahl, P. (1972), *Eur. J. Biochem. 25,* 20.

Brown, J. C., and Koshland, M. E. (1975), *Fed. Proc., Fed. Am. Soc. Exp. Biol. 34,* 971.

Cathou, R. E., and Dorrington, K. J. (1975), in *Biological Macromolecules Series,* Vol. 5, Part C, Timasheff, S., and Fasman, G., Ed., New York, N.Y., Marcel Dekker p 91.

Cathou, R. E., and Holowka, D. A. (1975), *Adv. Exp. Med. Biol. 64,* 207.

Cathou, R. E., Holowka, D. A., and Chan, L. M. (1974), *Prog. Immunol., Int. Congr. Immunol., 2nd, 1,* 63.

Chen, J. P., Reichlin, M., and Tomasi, T. B. (1969), *Biochemistry 8,* 2246.

Chen, R. F., and Bowman, R. L. (1965), *Science 147,* 1.

Colman, P. M., Deisenhofer, J., Huber, R., and Palm, W. (1976), *J. Mol. Biol. 100,* 257.

Crothers, D. M., and Metzger, H. (1972), *Immunochemistry 9,* 341.

Cunniff, R. V. H., Cole, H. H., and Stollar, B. D. (1968), *J. Immunol. 101,* 695.

Dale, R. E., and Eisinger, J. (1975), in Concepts in Biochemical Fluorescence, Vol. 1, Chen, R. F., and Edelhoch, H., Ed., New York, N.Y., Marcel Dekker p 115.

Deutsch, G., and Amiraian, K. (1968), *Immunology 15,* 623.

Dorrington, K. J., and Tanford, C. (1970), *Adv. Immunol. 12,* 333.

Edsall, J. T., and Mehl, J. W. (1943), in Proteins, Amino Acids, and Peptides, Edsall, J. T., and Cohn, C. A., Ed., New York, N.Y., Reinhold, p 406.

Ehrenberg, M., and Rigler, R. (1972), *Chem. Phys. Lett. 14,* 539.

Feinstein, A., Munn, E. A., and Richardson, N. E. (1971), *Ann. N.Y. Acad. Sci. 190,* 104.

Froese, A., and Sehon, A. H. (1975), *Immunochemistry 2,* 135.

Gottlieb, Y. Y., and Wahl, P. (1963), *J. Chem. Phys. 60,* 849.

Hester, R. B., Mole, J. E., and Schrohenloher, R. E. (1975), *J. Immunol. 114,* 486.

Holowka, D. A. (1975), Ph.D. Thesis, Tufts University, Medford, Mass.

Holowka, D. A., and Cathou, R. E. (1974), *Fed. Proc., Fed. Am. Soc. Exp. Biol. 33,* 1320.

Holowka, D. A., and Cathou, R. E. (1976), *Biochemistry,* preceding paper in this issue.

Isenberg, I., and Dyson, R. (1969), *Biophys. J. 9,* 1337.

Käiväräinen, A. I., Nezlin, R. S., Lichtenstein, H. I., Misharin, A. U., and Volkenstein, M. V. (1973), *Mol. Biol. (Moscow) 7,* 760.

Kim, Y. D., and Karush, F. (1973), *Immunochemistry 10,* 365.

Klapper, D. G., Clem, L. W., and Small, P. A., Jr. (1971), *Biochemistry 10,* 645.

Knopp, J. A., and Weber, G. (1969), *J. Biol. Chem. 244,* 6309.

Kunitz, I. D., Jr., and Kauzman, W. (1974), *Adv. Protein Chem. 28,* 239.

Li, Y.-H., Chan, L.-M., Tyer, L., Moody, R. T., Himel, C. M., and Hercules, D. M. (1975), *J. Am. Chem. Soc. 97,* 3118.

Lovejoy, C. F., Holowka, D. A., and Cathou, R. E. (1975), *Fed. Proc., Fed. Am. Soc. Exp. Biol. 34,* 544.

Marquardt, D. W. (1963), *J. Soc. Ind. Appl. Math. 11,* 431.

Metzger, H. (1970), *Adv. Immunol. 12,* 57.

Metzger, H. (1974), *Adv. Immunol. 18,* 169.

Metzger, H., Perlman, R. L., and Edelhoch, H. (1966), *J. Biol. Chem. 241,* 1741.

Noelken, M. E., Nelson, C. A., Buckley, C. E., and Tanford, C. (1965), *J. Biol. Chem. 240,* 218.

Parker, C. W., Yoo, T. J., Johnson, M. C., and Godt, S. M. (1967), *Biochemistry 6,* 3408.

Pilz, I., Kratky, O., Licht, A., and Sela, M. (1975), *Biochemistry 14,* 1326.

Plaut, A. G., and Tomasi, T. B., Jr. (1970), *Proc. Natl. Acad. Sci. U.S.A. 65,* 318.

Poljak, R. J., Amzel, L. M., Avery, H. P., Chen, B. L., Phizackarley, R. P., and Saul, F. (1973), *Proc. Natl. Acad. Sci. U.S.A. 70,* 3305.

Putnam, F. W., Florent, G., Paul, C., Shinoda, T., and Shimizu, A. (1973), *Science 182,* 287.

Rockey, J. H., Montgomery, P. C., Underdown, B. J., and Dorrington, K. J. (1972), *Biochemistry 11,* 3172.

Schlessinger, J., Steinberg, I. Z., and Pecht, I. (1974), *J. Mol. Biol. 87,* 725.

Shimizu, A., Watanabe, S., Yamamura, Y., and Putnam, F. W. (1974), *Immunochemistry 11,* 719.

Solheim, B. G., and Harboe, M. (1972), *Immunochemistry 9,* 623.

Stollar, B. D., Stadecker, M. J., and Morecki, S. (1976), *J. Immunol.,* (in press).

Svehag, S. E., Bloth, B., and Seligman, M. (1969), *J. Exp. Med. 130,* 691.

Tao, T. (1969), *Biopolymers 8,* 609.

Valentine, R. C., and Green, N. M. (1967), *J. Mol. Biol. 27,* 615.

Wahl, P., Kasai, M., and Changeux, J. P. (1971), *Eur. J. Biochem. 18,* 332.

Weber, G. (1952a), *Biochem. J. 51,* 145.

Weber, G. (1952b), *Biochem. J. 51,* 155.

Werner, T. C., Bunting, J. R., and Cathou, R. E. (1972), *Proc. Natl. Acad. Sci. U.S.A. 69,* 795.

Witholt, B., and Brand, L. (1970), *Biochemistry 9,* 1948.

Yguerabide, J. (1972), *Methods Enzymol. 26C,* 498.

Yguerabide, J., Epstein, H. F., and Stryer, L. (1970), *J. Mol. Biol. 51,* 573.

Zagyansky, Y. A. (1975), *Arch. Biochem. Biophys. 166,* 371.

Zagyansky, Y. A., and Ivannikova, E. I. (1974), *Mol. Biol. Rep. 1,* 301.

Zagyansky, Y. A., Tumerman, L. A., and Egorov, A. M. (1972), *Immunochemistry 9,* 91.

Zikăn, J., and Miler, I. (1974), *Immunochemistry 11,* 115.